Magnetic field generation by intermittent convection

R. Chertovskih[a,b,*], E.L. Rempel[c,d], E.V. Chimanski[c]

[a] *Research Center for Systems and Technologies, Faculty of Engineering, University of Porto, Rua Dr. Roberto Frias, s/n, Porto 4200–465, Portugal*
[b] *Samara National Research University, Moskovskoye Shosse 34, Samara 443086, Russian Federation*
[c] *Aeronautics Institute of Technology, São José dos Campos, São Paulo 12228–900, Brazil*
[d] *National Institute for Space Research and World Institute for Space Environment Research, São José dos Campos, São Paulo 12227–010, Brazil*

Abstract

Magnetic field generation in three-dimensional Rayleigh-Bénard convection of an electrically conducting fluid is studied numerically by fixing the Prandtl number at $P = 0.3$ and varying the Rayleigh number (Ra) as a control parameter. A recently reported route to hyperchaos involving quasiperiodic regimes, crises and chaotic intermittent attractors is followed, and the critical magnetic Prandtl number (P_m^c) for dynamo action is determined as a function of Ra. A mechanism for the onset of intermittency in the magnetic energy is described, the most beneficial convective regimes for dynamo action in this transition to weak turbulence are identified, and the impact of intermittency on the dependence of P_m^c on Ra is discussed.

Keywords: Magnetohydrodynamics, Rayleigh-Bénard convection, convective dynamo, intermittency.

1. Introduction

Thermal convection plays an important role in magnetic field generation in planets and stars. For instance, the Earth's magnetic field is sustained by a dynamo process driven by convective flows in the liquid iron outer core, whereby

*Corresponding author
Email address: roman@ssau.ru (R. Chertovskih)

thermal energy is transformed into kinetic energy and then into magnetic field energy. The fluid motions are driven by buoyancy forces and are strongly affected by the Lorentz force, due to the strength of the Earth's magnetic field in the core, as well as the Coriolis force, due to the Earth's rotation [1]. Historical data on geomagnetic field evolution based on the paleomagnetic record that can form in rocks reveal nonperiodic intermittent time series, both for the field intensity and for the frequency of polarity reversals [2]. By intermittent, we mean that the field undergoes recurrent and aperiodic switching between two qualitatively different states. Thus, the geomagnetic field randomly alternates between stronger ("bursty") and weaker ("laminar") phases. The relation between the field intensity and the frequency of reversals is still not clear. For instance, Prévot *et al.* [3] conjectured that the Mesozoic dipole low corresponded roughly to a progressive decrease in the average frequency of reversals, which contrasts with more recent data that indicate that the time-averaged field has been higher during periods without reversals in the past two million years, whereas more reversals are expected during periods of weak field intensity [4]. In fact, there may be no simple correlation between reversal rate and intensity [5], but overall the geodynamo seems to exhibit a strongly chaotic/intermittent rather than periodic behavior. Intermittency is also observed in the solar magnetic activity as recorded by the grand minima of the sunspots cycle [6].

Several numerical experiments have tried to capture the chaotic intermittent features of the geomagnetic and solar dynamos. The main difficulty in such studies is that a dynamo mechanism cannot sustain an axisymmetric magnetic field, due to Cowling's anti-dynamo theorem [7], therefore, fully three-dimensional models have to be employed for a self-consistent simulation. Both global (spherical) [8, 9, 10] or local (planar) [11, 12] three-dimensional convective models have been used. However, parameter values corresponding to the planetary and stellar interiors require a huge amount of computations which cannot be performed even on modern high performance computers in a reasonable time.

A set of dimensionless parameters has been defined to describe convective dynamos. Some of them are the Rayleigh number (Ra), that measures the mag-

nitude of the thermal buoyancy force, the Prandtl number (P), which is the ratio of kinematic viscosity to thermal diffusivity, and the magnetic Prandtl number (P_m), defined as the ratio between kinematic viscosity and magnetic diffusivity. One of the main problems in dynamo theory is to determine the relation between the values of those parameters and the onset of dynamo action. For a review of scaling properties of convective–driven dynamo models in rotating spherical shells, see [13]. Here, we are interested in magnetic field generation in Rayleigh-Bénard convection (RBC) for moderately low Prandtl number (the Prandtl number in the Earth's outer core has been estimated to be between 0.1 and 0.5 [14, 15]). In this context, strong dependence of the magnetic fields generated by convective flows on the value of the Prandtl number was found for $0.2 \leq P \leq 5$ [16]. Analysis of the kinematic dynamo problem by Podvigina [17] showed that convective attractors for $P = 0.3$ favour the magnetic field generation in comparison to the attractors found for larger values of P ($P = 1$ and $P = 6.8$). In recent multiscale analysis of the RBC dynamo problem in the presence of rotation [18], low Prandtl number convection was also found to be beneficial for magnetic field generation. In the present work, we follow our recently published analysis of transition to chaos and hyperchaos in RBC as a function of the Rayleigh number for $P = 0.3$ [19]. Chaotic systems are characterized by aperiodic motions that are sensitive to initial conditions, i.e., close initial conditions tend to locally diverge exponentially with time, with the mean divergence rate measured by a positive maximum Lyapunov exponent. In hyperchaos a system presents more than one positive Lyapunov exponent, implying that divergence occurs in more than one direction among a set of orthogonal directions in the phase space. As the number of positive exponents increases, the resulting dynamics becomes more irregular in space and time, thus, hyperchaotic systems have been termed weakly turbulent [20]. We assume the fluid to be electrically conducting and add an initial seed magnetic field to investigate the onset of dynamo. The intermittency in the velocity field described in ref. [19] as being due to global bifurcations constitutes the starting point for our search for an explanation for the intermittent dynamo. We stress

that our hydrodynamic regimes are in a transition state between weak chaos and turbulence, therefore, the system displays a complex switching between highly different phases that is typically very difficult to be studied, since the convergence of average quantities is much slower than in fully developed turbulence, and the meaning of those averages may be rather deceptive if they do not take into account information about the different phases of the flow.

Usually, large Rayleigh numbers are beneficial for magnetic field generation in spherical shells simulations [21], *i.e.*, the critical P_m for dynamo action decreases with increasing Ra. For moderate values of Ra, in Calkins *et al.* [18] a similar dependence in plane layer dynamos was found, while in refs. [17, 22] it is reported that for Ra beyond a certain threshold the behaviour of the critical P_m ceases to be monotonic. In this work we describe a scenario where the non-monotonic behaviour of the critical P_m is explained based on an analysis of the intermittency in the convective attractors. Thus, our goals are threefold: *i*) to explain a mechanism for intermittency in magnetic field fluctuations in RBC; *ii*) to describe how this type of intermittency is responsible for the non-monotonic behaviour of the critical P_m as a function of Ra and *iii*) to detect what are the best hydrodynamic regimes for magnetic field amplification, that is, the regimes where dynamo action takes place for smaller P_m, among the hydrodynamic attractors in the RBC system in transition to turbulence.

2. Statement of the problem and solution

We consider a newtonian incompressible fluid flow in a horizontal plane layer; the fluid is electrically conducting and uniformly heated from below and cooled from above. Fluid flow is buoyancy-driven and the Boussinesq approximations (see, *e.g.*, [23]) are assumed. In a Cartesian reference frame with the orthonormal basis $(\mathbf{e}_1, \mathbf{e}_2, \mathbf{e}_3)$, where $\mathbf{e}_3$ is opposite to the direction of gravity,

the equations governing the magnetohydrodynamic (MHD) system are [24]:

$$\frac{\partial \mathbf{v}}{\partial t} = P\nabla^2\mathbf{v} + \mathbf{v}\times(\nabla\times\mathbf{v}) - \mathbf{b}\times(\nabla\times\mathbf{b}) + P\mathrm{Ra}\theta\mathbf{e}_3 - \nabla p, \tag{1}$$

$$\frac{\partial \mathbf{b}}{\partial t} = \frac{P}{P_m}\nabla^2\mathbf{b} + \nabla\times(\mathbf{v}\times\mathbf{b}), \tag{2}$$

$$\frac{\partial \theta}{\partial t} = \nabla^2\theta - (\mathbf{v}\cdot\nabla)\theta + v_3, \tag{3}$$

$$\nabla\cdot\mathbf{v} = 0, \tag{4}$$

$$\nabla\cdot\mathbf{b} = 0, \tag{5}$$

where $\mathbf{v}(\mathbf{x},t) = (v_1, v_2, v_3)$ is the fluid velocity, $\mathbf{b}(\mathbf{x},t) = (b_1, b_2, b_3)$ the magnetic field, $p(\mathbf{x},t)$ the pressure, $\theta(\mathbf{x},t)$ is the difference between the flow temperature and the linear temperature profile; the spatial coordinates are $\mathbf{x} = (x_1, x_2, x_3)$ and t stands for time. The non-dimensional parameters are the Prandtl number, $P = \nu/\kappa$, the magnetic Prandtl number, $P_m = \nu/\eta$, and the Rayleigh number, $\mathrm{Ra} = \alpha g \delta T d^3/(\nu\kappa)$, where ν is the kinematic viscosity, κ the thermal diffusivity, η the magnetic diffusivity, α the thermal expansion coefficient, g the gravity acceleration, δT the temperature difference between the layer boundaries, and d the vertical size of the layer. The units of length and time are d and the vertical heat diffusion time, d^2/κ, respectively; $\mathbf{v}$, $\mathbf{b}$ and θ are measured in units of κ/d, $\sqrt{\mu_0\rho}\kappa/d$ and δT, respectively. Here μ_0 stands for the vacuum magnetic permeability and ρ the mass density.

The horizontal boundaries of the plane layer, $x_3 = 0$ and $x_3 = 1$, are assumed to be stress-free, $\partial v_1/\partial x_3 = \partial v_2/\partial x_3 = v_3 = 0$, electrically perfectly conducting, $\partial b_1/\partial x_3 = \partial b_2/\partial x_3 = b_3 = 0$, and maintained at constant temperatures, $\theta = 0$. A square convective cell is considered, $\mathbf{x} \in [0, L]^2 \times [0, 1]$, all the fields are periodic in the horizontal directions, x_1 and x_2, with period L.

We study magnetic field generation by the hyperchaotic convective attractors found in [19] for $L = 4$, $P = 0.3$ and $2160 \leq \mathrm{Ra} \leq 5000$ (the critical Rayleigh number for the onset of convection is $\mathrm{Ra_c}$=657.5 [23]). For a given value of Ra, the initial condition for the hydrodynamic part of the system, $\mathbf{v}(\mathbf{x}, 0)$ and

$\theta(\mathbf{x}, 0)$, is taken from the corresponding convective attractor; the initial magnetic field is $\mathbf{b}(\mathbf{x}, 0) = (\cos(\pi x_2/2), 0, 0)$ scaled such that the magnetic energy $E_b(0) = 10^{-7}$. For each convective attractor the governing equations (1)–(5) are integrated forward in time for a certain value of P_m in order to estimate the critical magnetic Prandtl number, P_m^c. Thus, if $P_m > P_m^c$ the magnetic field is maintained in the system (dynamo), for $P_m < P_m^c$, the magnetic field decays (no dynamo). We consider values of P_m from 1 to 10 with step 1; the value is regarded to be subcritical if $E_b(t) < 10^{-50}$ for a time interval greater than 500, otherwise it is supercritical and the generated magnetic field is analysed.

For a given initial condition, equations (1)–(5) are integrated numerically using the standard pseudospectral method [25]: the fields are represented as Fourier series in all spatial variables (exponentials in the horizontal directions, sine/cosine in the vertical direction), derivatives are computed in the Fourier space, multiplications are performed in the physical space, and the Orszag 2/3-rule is applied for dealiasing. The system of ordinary differential equations for the Fourier coefficients is solved using the third-order exponential time-differencing method ETDRK3 [26] with constant step $5 \cdot 10^{-4}$. At each time step the fields $\mathbf{v}$ and $\mathbf{b}$ are projected onto space of solenoidal functions by solving the Poisson equation in the Fourier space. Spatial resolution is $86 \times 86 \times 43$ Fourier harmonics (multiplications were performed on a uniform $128 \times 128 \times 64$ grid). For all solutions, time-averaged energy spectra of the magnetic and velocity fields decay as a function of the wavenumber at least by 3 and 7 orders of magnitude, respectively. Several simulations with the doubled resolution showed no significant change in the results. In computations we traced the kinetic, $E_v(t)$, and magnetic, $E_b(t)$, energies, which are the L_2 norm of the squared field normalized by the volume of the convective cell. We also computed the critical magnetic Reynolds number, $\mathrm{Re}_\mathrm{m}^\mathrm{c} = P_m^c L\sqrt{< E_v >}/P$, where angle brackets stand for time-averaging.

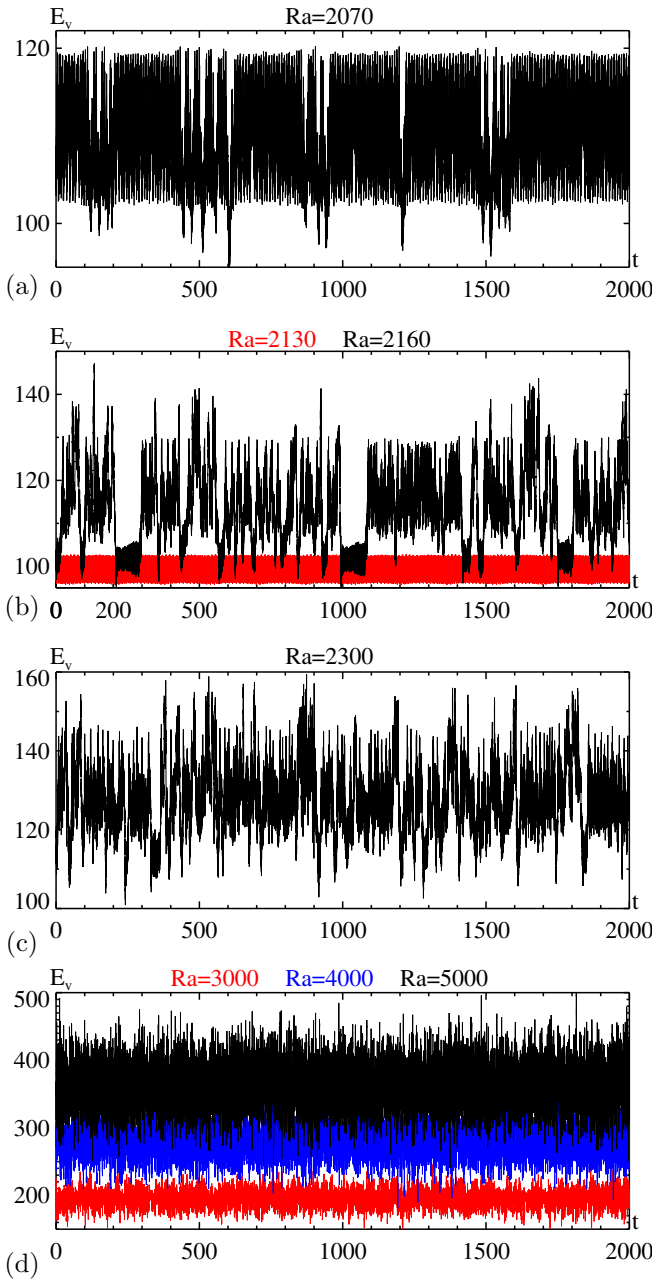

Figure 1: (Color online) Evolution of the kinetic energy in the absence of magnetic field for the attractors of the convective system at Ra=2070 (a), 2130, 2160 (b), 2300 (c) 3000, 4000 and 5000 (d).

Table 1: Types of the convective attractors considered in the paper, ratio of the Rayileigh number to its critical value at the onset of convection; the critical values of the magnetic Prandtl number, P_m^c, and the corresponding critical magnetic Reynolds number, $\mathrm{Re_m^c}$, computed for the middle value of P_m^c in the corresponding interval.

Ra	$\mathrm{Ra/Ra_c}$	Type	P_m^c	$\mathrm{Re_m^c}$
2070	3.1	chaotic	$9 < P_m^c < 10$	1320
2130	3.2	quasiperiodic	$2 < P_m^c < 3$	332
2160	3.3	hyperchaotic	$6 < P_m^c < 7$	922
2300	3.5	hyperchaotic	$7 < P_m^c < 8$	1129
3000	4.6	hyperchaotic	$8 < P_m^c < 9$	1584
4000	6.1	hyperchaotic	$6 < P_m^c < 7$	1453
5000	7.6	hyperchaotic	$5 < P_m^c < 6$	1399
6000	9.1	hyperchaotic	$4 < P_m^c < 5$	1269

3. Results

The present work studies magnetic field generation by the branch of hyperchaotic attractors of the convective system for Ra $\geq$ 2140 [19]. This branch is formed in an interior crisis, whereby a quasiperiodic attractor collides with a background nonattracting chaotic set (a chaotic saddle) to form an enlarged chaotic attractor, where trajectories intermittently switch between the former quasiperiodic attractor and the surrounding chaotic saddle. In what follows we briefly describe the convective regimes in the absence of magnetic field in this interval of Ra, also mentioning the pre-crisis attractors at Ra=2070 and Ra=2130 (see [19] for more details); the considered values of Ra and the temporal behaviour of the corresponding hydrodynamic attractors are summarized in table 1.

3.1. Convective states

In the absence of magnetic field, the convective regime for Ra=2070 is chaotic (see fig. 1(a)). This convective state loses its stability for Ra $>$ 2070, originating

the chaotic saddle mentioned above. For Ra=2130, the sole attractor in the convective system is quasiperiodic with three incommensurate time frequencies. The evolution of its kinetic energy is shown in fig. 1(b)(red line) and in what follows it is referred to as the regular (convective) state. For Ra$\geq$ 2140, its stability is lost, and a new hyperchaotic attractor rises as the sole attractor of the convective system. Its intermittent nature near its birth is revealed by the kinetic-energy time series (see fig. 1(b)(black line) for the attractor at Ra=2160). The trajectory in the phase space visits the destabilized regular state at, *e.g.*, $200 \leq t \leq 300$ and $1000 \leq t \leq 1100$, as well as bursty chaotic phases related to the destabilized chaotic attractor (compare the energy levels of the bursty phases of figs. 1(b)(black line) and 1(a)). The average time spent near the regular state is shortened for increasing Ra (cf. Ra=2160 in fig. 1(b) and Ra=2300 in fig. 1(c); see also fig. 6 in [19]). For Ra $\geq$ 3000 the laminar phases in the intermittency are no longer recognizable at the time scale shown (see the kinetic energy evolution for attractors at Ra=3000, 4000 and 5000 in fig 1(d)). The absence of regular phases is to be expected, since those phases are shortened as one moves away from the interior crisis point at Ra $\approx$ 2140 [27].

3.2. Magnetic field generation

The critical magnetic Prandtl number, P_m^c, for the chaotic convective attractor at Ra=2070 is $9 < P_m^c < 10$ (see fig. 2(a)), while for the regular state at Ra=2130, it is $2 < P_m^c < 3$ (see fig. 3(a)). This significant difference in P_m^c is crucial for the onset of magnetic field generation by the convective attractors for larger values of Ra, where both regular and bursty phases are destabilized, but visited intermittently.

At Ra=2070, for the supercritical value $P_m = 10$, after an initial exponential growth the magnetic field generated by the convective attractor reaches a chaotic state with a relatively small fluctuation (see fig. 2(a), upper red line). In this transition to the saturated MHD state, the kinetic energy undergoes a significant decrease (black line in fig. 2(a)). In the saturated state, a dominant spatial feature of magnetic fields is its concentration in half-ropes located near the

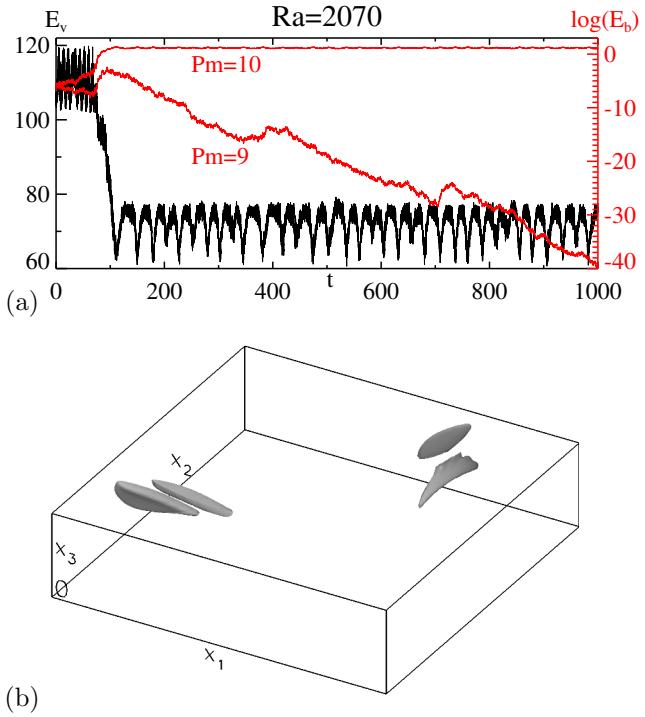

Figure 2: (Color online) (a): Evolution of the kinetic (black line, left axis) and logarithm of the magnetic (red line, right axis, non-decaying in time) energies for the convective attractor at Ra=2070 and $P_m = 10$. Magnetic energy decay for the same Ra and $P_m = 9$ is represented by the lower red line. (b): Snapshot at $t = 400$ of isosurfaces of magnetic energy density, at a level of a third of the maximum, for the MHD state at Ra=2070 and $P_m = 10$ shown in (a); one periodicity cell is displayed.

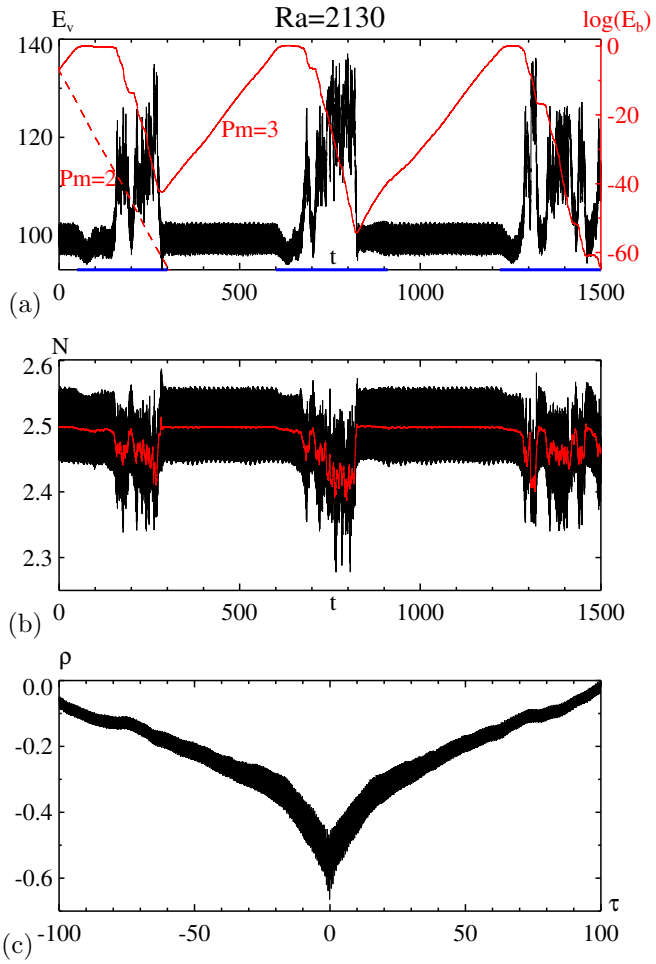

Figure 3: (Color online) (a): Evolution of the kinetic, $E_v(t)$, (black line, left axis) and logarithm of magnetic, $E_b(t)$, (red line, right axis) energies for the convective attractor at Ra=2130 and $P_m = 3$. Thick blue lines in the horizontal axis represent time intervals, where the trajectory in the phase space is in transition before recovering the convective attractor. Magnetic energy evolution for the same Ra and $P_m = 2$ is represented by the red dashed line. (b): Evolution of the spectral average, $N(t)$, (black line) and its forward moving average over time interval of length 2 (red line) for the regime at Ra=2130 and $P_m = 3$ shown in (a). (c): Cross correlation, $\rho(\tau)$, of the kinetic energy shown in (a) and the spectral average shown in (b); τ stands for lag measured in units of time.

horizontal boundaries (see a snapshot of isosurfaces of magnetic energy density, $(\mathbf{b} \cdot \mathbf{b})/2$, in fig. 2(b)). This feature is common for all magnetohydrodynamic regimes found in the paper; such configuration of magnetic field was observed in many convective dynamo simulations with perfectly electrically conducting boundaries (see, e.g., [11, 28]).

The magnetic field generated by the regular convective attractor at Ra=2130 and $P_m = 3$ is represented in fig. 3(a), and shows a very different behaviour. After the initial exponential growth ($0 \leq t \leq 50$), the magnetic field saturates at $0.3 \leq E_b(t) \leq 1.6$ for $50 \leq t \leq 160$. Affected by the stronger magnetic field, the perturbed convective attractor loses its previously laminar behaviour and undergoes a chaotic burst. During the burst, it ceases to generate magnetic field and for $160 \leq t \leq 290$ the magnetic energy decreases by 42 orders of magnitude. At $t \approx 280$ the magnetic energy is low enough so that the unperturbed regular convective attractor is recovered and the magnetic field gets reamplified by dynamo action. This scenario repeats intermittently in time. The time to recover the convective attractor from the magnetic perturbation varies significantly: in fig. 3(a) it is 250 time units (from $t = 50$ to $t = 300$) and 310 (from $t = 600$ to $t = 910$) (these time intervals are illustrated by thick blue lines in the horizontal axis). An interesting feature of this magnetohydrodynamic regime is that the magnetic field is generated by a less energetic and more regular (in time) phase.

This intermittent switching between the amagnetic (hydrodynamic) and the magnetic states can be named as a "self-killing-and-self-recreating" dynamo, in contrast to the "self-killing" dynamos [29], where the generated magnetic field modifies the flow in such a way that it is attracted to a non-generating stable hydrodynamic state. Similar, although periodic in time, switching between a generating steady hydrodynamic state and an unstable steady MHD state was found in [11] (see fig. 22 *ibid.*), where magnetic field generation in the rotating RBC was studied at various rotation rates.

The intermittent convective attractor for Ra=2160 (see fig. 1(b)) does not generate magnetic field for $P_m \leq 6$. For $P_m = 7$, the generated magnetic field inherits the intermittent behaviour from the flow – when the regime is near the

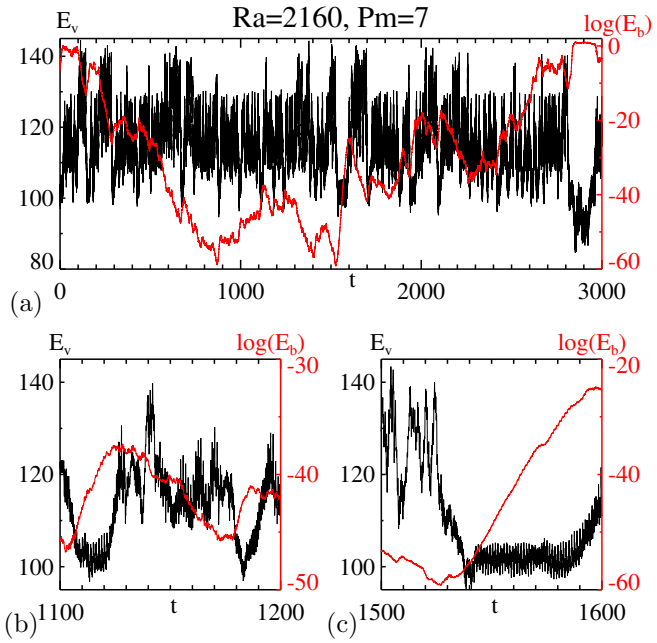

Figure 4: (Color online) Evolution of the kinetic (black line, left axis) and logarithm of magnetic (red line, right axis) energies for the convective attractor at Ra=2160. Full time interval is shown in (a) and two time windows are represented in (b) and (c).

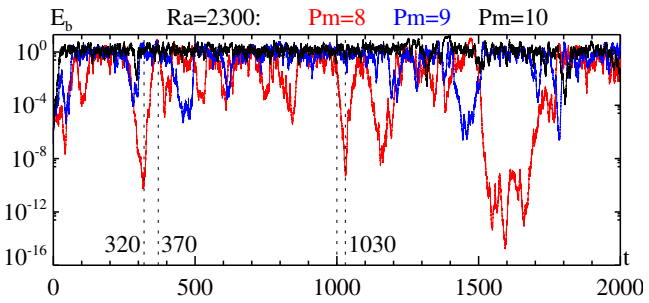

Figure 5: (Color online) Evolution of the magnetic energy generated by the convective attractor at Ra=2300 and for $P_m = 8$ (red), $P_m = 9$ (blue) and $P_m = 10$ (black).

regular state, the magnetic field is amplified (see fig. 4 (b) in $1105 \leq t \leq 1130$ and (c) in $1530 \leq t \leq 1600$); when the state is near the bursty phases, the magnetic field is decaying (see fig. 4 (b) in $1130 \leq t \leq 1170$). In contrast to the case at Ra=2130, here the origin of the transition from the regular to the bursty state is not the influence of the generated magnetic field, but the intrinsic intermittency due to the instability of both states in the purely hydrodynamic regime.

Figure 5 shows the time series of the magnetic energy at Ra=2300 for different values of P_m. For the slightly supercritical value $P_m = 8$ (red line), it displays intermittency, with an interplay of the regular states amplifying the magnetic field (e.g. for $320 \leq t \leq 370$) and bursty states suppressing its generation (e.g. for $1000 \leq t \leq 1030$). The amplitude of magnetic energy variation is 16 orders of magnitude. The generated magnetic field is weak, as well as its influence on the flow, so the dynamo is subordinated to the switching between the regular and irregular phases of the convective regime. On increasing P_m to 9 (blue line), and then 10 (black line), the fluctuations of the magnetic energy become smaller. Since larger values of P_m with fixed P correspond to weaker magnetic diffusion, the stronger magnetic fields bring the resulting MHD regimes farther from the hydrodynamic one.

The same estimate of P_m^c and the same behaviour of the generated magnetic field near onset extends to the convective attractors at Ra=2400 and 2500.

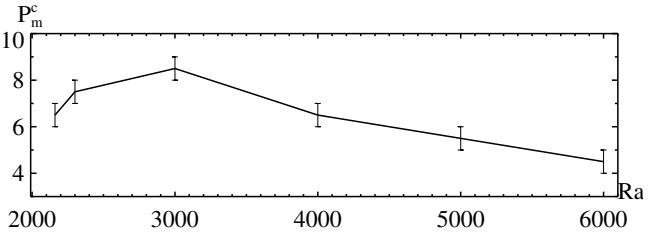

Figure 6: Dependence of the critical magnetic Prandtl number estimate on Ra for the hyperchaotic regimes.

For the convective attractor at Ra=3000 the critical magnetic Prandtl number achieves its maximal value along the considered hyperchaotic convective regimes, $8 < P_m^c < 9$. On further increase of Ra, for the sequence of convective attractors at Ra $= 3000, 4000, 5000$ and 6000, where the regular phases are no longer seen, the critical magnetic Prandtl number decreases with Ra (see table 1 and fig. 6). Simulations with the doubled resolution confirm this tendency for much higher values of Ra. This is in accordance with findings referred in Busse [21] for large values of Ra.

In order to understand why the quiescent phases of the kinetic energy time series correspond to better dynamos, we characterized the hydrodynamic states by a measure of the number of active spatial Fourier modes. The spectral average has been frequently employed in this context [30], being defined as

$$N(t) = \sqrt{\sum_{n=1}^{\infty} \sum_{\mathbf{k} \in C_n} |\mathbf{k}|^2 |\hat{\mathbf{v}}_{\mathbf{k}}(t)|^2 / \sum_{n=1}^{\infty} \sum_{\mathbf{k} \in C_n} |\hat{\mathbf{v}}_{\mathbf{k}}(t)|^2}$$

where $\hat{\mathbf{v}}_{\mathbf{k}}$ denotes the kth Fourier coefficient of the velocity field, and $C_n = \{\mathbf{k} \colon n - 1 < |\mathbf{k}| \leq n\}$ stands for the nth ($n \in \mathbb{N}$) spherical shell in the space of Fourier wave vectors $\mathbf{k}$. Note that the spectral average is the square root of the averaged $|\mathbf{k}|^2$, where the average is weighted by the shell-integrated energy. Therefore, it measures the energy spread in the $\mathbf{k}$ spectrum, and should increase with time in systems with energy cascade until dissipative effects restrain its growth. It can also be seen as the square-root of the ratio of the enstrophy to the energy and, consequently, as the inverse of a length scale related to viscous

dissipation. We employ the spectral average $N(t)$ as a measure of the effective number of degrees of freedom in the convective system.

Fig. 7 plots the time series of $N(t)$ for some of the hydrodynamic regimes of fig. 1. Note that the chaotic attractor at Ra=2070 has lower average $N(t)$ than the quasiperiodic attractor at Ra=2130; consequently, the regular phases in the intermittent series at Ra=2160 display higher $N(t)$ than the bursty phases. The higher values of $N(t)$ found in the quiescent phases correlates well with the periods of magnetic field growth (for the same regime at Ra=2130 and $P_m = 3$ cf. evolution of the kinetic and magnetic energies in fig. 3(a) with the spectral average, $N(t)$, in (b); in order to demonstrate the negative correlation of the kinetic energy and the spectral average the cross correlation function of these quantities, $\rho(\tau)$, is shown in (c)). For higher values of Ra (two lower panels of fig. 7), the system dynamics is strongly irregular and the average $N(t)$ becomes larger, which coincides with the monotonic decay of the critical P_m for dynamo action in these cases.

4. Conclusions

We have shown how intermittent convective attractors with two or more qualitatively different (quiescent and bursty) phases can lead to intermittent dynamo action. The critical P_m for dynamo action is lower for the quasiperiodic/quiescent attractors compared to the hyperchaotic/bursty attractors. As Ra is increased, the quiescent phases in the intermittent time series are shortened and, thus, the overall critical P_m also becomes larger due to the predominance of bursts in the time series. Further increase in Ra leads the convective system to a state where quiescent phases are no longer observable and, then, the critical P_m starts to decrease with increasing Ra, as expected in strongly hyperchaotic/turbulent systems. Therefore, in transition to turbulence, quasiperiodic states are preferred for dynamo action in the intermittent regimes, but in stronger chaotic regimes without this type of chaotic intermittency, the critical P_m is expected to become lower and lower as Ra is increased. This low-P_m

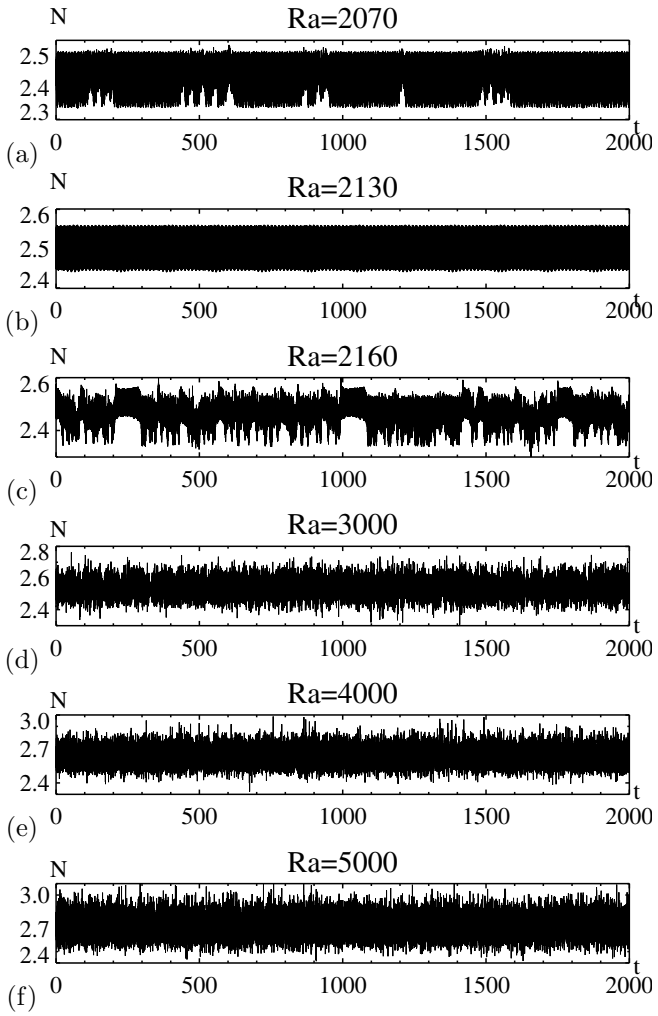

Figure 7: Time series of the spectral average $N(t)$ for the convective attractors in the absence of magnetic field for Ra=2070 (a), 2130 (b), 2160 (c), 3000 (d), 4000 (e) and 5000 (f).

MHD regime is of particular interest, since many geophysical and astrophysical problems are described by low P_m. For example, in the Sun, P_m varies between 10^{-7} and 10^{-4} between the top and the bottom of the convection zone [31], whereas in the geodynamo it is approximately 5×10^{-6} [32].

The intermittent switching between qualitatively different phases in the time series of kinetic energy shown in figs. 1 and 3(a) resembles the bi-stability reported by Zimmerman *et al.* [33] in experiments with a rotating spherical Couette flow and later associated with the intermittent behavior of the magnetic field in an MHD experiment with an imposed magnetic field [34]. For instance, fig. 10 of ref. [34] shows time series of torque and azimuthal magnetic field where the system undergoes intermittent transitions between two phases with very different mean values. The intermittency in our magnetic energy time series also shows similarity with the on-off intermittent ABC-flow dynamo reported by Rempel *et al.* [30], where the magnetic energy time series intercalate bursty phases with quiescent phases of almost null magnetic energy. This type of intermittency is expected to happen near critical values of the control parameters where a global bifurcation in the underlying attractor takes place [35, 36], and has recently been found in numerical simulations of rotating spherical Couette flows with realistic boundary conditions [37].

The verification that the quasiperiodic quiescent phases of the velocity field constitute a better dynamical state for a convective dynamo than the bursty phases for low Ra may seem at odds with the intuitive idea that a chaotic flow should favor the stretching, twisting and folding (STF) of magnetic field lines, which is a well known mechanism for magnetic field amplification [38]. However, one should note that the STF dynamo may operate even in stationary flows with chaotic streamlines. Inhibition of the large-scale magnetic field by large fluctuations of the velocity field is shown analytically in [39] for some simple flows using the mean-field dynamo theory. In our case, we have shown that the quiescent/regular phases in the intermittent regime excite a higher number of spatial Fourier modes than the bursty phases, which implies the increase in magnetic flux in the regular phases. For higher values of Ra, when the energy

cascade and spatiotemporal complexity increase, the critical P_m decreases. It would be interesting to check if the same happens in spherical geometries, in a set up more closely related to the difficult task of magnetic field generation in laboratory experiments. As a final remark, it is worth mentioning that the behavior of the dynamo can be quite different in the presence of rotation and that should be the topic of future exploration.

Acknowledgments

RC, ELR and EVC acknowledge financial support from FAPESP (2013/01242-8, 2013/26258-4 and 2016/07398-8, respectively). RC was partially financed by the project POCI–01–0145–FEDER–006933 SYSTEC funded by FEDER funds through COMPETE 2020 and by FCT (Portugal). ELR also acknowledges financial support from CNPq (grant 305540/2014-9) and CAPES (grant 88881.068051/2014-01).

[1] K. Zhang, Nonlinear magnetohydrodynamic convective flows in the Earth's fluid core, Phys. Earth Planet. Inter. 111 (1–2) (1999) 93–103.

[2] M. Y. Reshetnyak, V. E. Pavlov, Evolution of the dipole geomagnetic field. Observations and models, Geomagn. Aeron. 56 (1) (2016) 110–124.

[3] M. Prévot, M. E.-M. Derder, M. McWilliams, J. Thompson, Intensity of the Earth's magnetic field: evidence for a Mesozoic dipole low, Earth Planet. Sci. Lett. 97 (1) (1990) 129–139.

[4] J.-P. Valet, L. Meynadier, Y. Guyodo, Geomagnetic dipole strength and reversal rate over the past two million years, Nature 435 (7043) (2005) 802–805.

[5] R. Heller, R. T. Merrill, P. L. McFadden, The variation of intensity of earth's magnetic field with time, Phys. Earth Planet. Inter. 131 (3) (2002) 237–249.

[6] J. Beer, S. Tobias, N. Weiss, An active Sun throughout the Maunder minimum, Sol. Phys. 181 (1998) 237.

[7] T. G. Cowling, The magnetic field of sunspots, Mon. Not. Roy. Astron. Soc. 94 (1) (1933) 39–48.

[8] G. A. Glatzmaier, R. S. Coe, L. Hongre, P. H. Roberts, The role of the Earth's mantle in controlling the frequency of geomagnetic reversals, Nature 401 (1999) 885–890.

[9] P. Olson, P. Driscoll, H. Amit, Dipole collapse and reversal precursors in a numerical dynamo, Phys. Earth Planet. Inter. 173 (1–2) (2009) 121–140.

[10] R. Raynaud, S. M. Tobias, Convective dynamo action in a spherical shell: symmetries and modulation, J. Fluid Mech. 799 (2016) R6.

[11] R. Chertovskih, S. Gama, O. Podvigina, V. Zheligovsky, Dependence of magnetic field generation by thermal convection on the rotation rate: a case study, Physica D 239 (13) (2010) 1188–1209.

[12] M. Calkins, K. Julien, S. Tobias, J. Aurnou, A multiscale dynamo model driven by quasi-geostrophic convection, J. Fluid Mech. 780 (2015) 143–146.

[13] U. R. Christensen, J. Aubert, Scaling properties of convection-driven dynamos in rotating spherical shells and application to planetary magnetic fields, Geophys. J. Int. 166 (1) (2006) 97–114.

[14] P. Olson, Overview, in: G. Schubert (Ed.), Treatise on Geophysics, Volume 8: Core Dynamics, Elsevier, 2007, pp. 1–30.

[15] D. Fearn, P. Roberts, Mathematical aspects of natural dynamos, in: E. Dormy, A. Soward (Eds.), The geodynamo, Roca Baton: CRC Press, 2007.

[16] T. Šoltis, J. Šimkanin, Hydromagnetic dynamos in rotating spherical fluid shells in dependence on the Prandtl number, density stratification and elec-

tromagnetic boundary conditions, Contrib. to Geophys. and Geodesy 44 (4) (2014) 293–312.

[17] O. M. Podvigina, Magnetic field generation by convective flows in a plane layer: the dependence on the Prandtl numbers, Geophys. Astrophys. Fluid Dyn. 102 (4) (2008) 409–433.

[18] M. A. Calkins, K. Julien, S. M. Tobias, J. M. Aurnou, P. Marti, Convection-driven kinematic dynamos at low Rossby and magnetic Prandtl numbers: single mode solutions, Phys. Rev. E 93 (2016) 023115.

[19] R. Chertovskih, E. Chimanski, E. Rempel, Route to hyperchaos in Rayleigh-Bénard convection, Europhys. Lett. 112 (2015) 14001.

[20] P. Manneville, Rayleigh-Bénard convection: thirty years of experimental, theoretical, and modeling work, in: I. Mutabazi, J. E. Wesfreid, E. Guyon (Eds.), Dynamics of Spatio-temporal Cellular Structures, Springer, 2006, pp. 41–65.

[21] F. Busse, Homogeneous dynamos in planetary cores and in the laboratory, Annu. Rev. Fluid Mech. 32 (2000) 383–408.

[22] O. Podvigina, Magnetic field generation by convective flows in a plane layer, Eur. Phys. J. B 50 (2006) 639–652.

[23] S. Chandrasekhar, Hydrodynamic and Hydromagnetic Stability, Dover, 1961.

[24] M. Meneguzzi, A. Pouquet, Turbulent dynamos driven by convection, J. Fluid Mech. 205 (1989) 297–318.

[25] C. Canuto, M. Hussaini, A. Quarteroni, T. Zang, Spectral Methods: Fundamentals in Single Domains, Springer, 2006.

[26] S. M. Cox, P. C. Matthews, Exponential time differencing for stiff systems, J. Comput. Phys. 176 (2) (2002) 430–455.

[27] C. Grebogi, E. Ott, F. Romeiras, J. A. Yorke, Critical exponents for crisis-induced intermittency, Phys. Rev. A 36 (11) (1987) 5365.

[28] M. St Pierre, The strong field branch of the Childress-Soward dynamo, in: M. R. E. Proctor, P. C. Matthews, A. M. Rucklidge (Eds.), NATO Advanced Study Institute: Solar and Planetary Dynamos, Cambridge University Press, 1993, pp. 295–302.

[29] H. Fuchs, K.-H. Rädler, M. Rheinhardt, On self-killing and self-creating dynamos, Astro. Nachr. 320 (1999) 129.

[30] E. L. Rempel, M. R. E. Proctor, A. C.-L. Chian, A novel type of intermittency in a non-linear dynamo in a compressible flow, Mon. Not. Roy. Astron. Soc. 400 (1) (2009) 509–517.

[31] A. Brandenburg, The solar interior – radial structure, rotation, solar activity cycle, in: A. C.-L. Chian, Y. Kamide (Eds.), Handbook of the Solar-Terrestrial Environment, Springer, 2007, pp. 27–54.

[32] M. Kono, P. H. Roberts, Recent geodynamo simulations and observations of the geomagnetic field, Rev. Geophys. 40 (2002) 1013.

[33] D. S. Zimmerman, S. A. Triana, D. P. Lathrop, Bi-stability in turbulent, rotating spherical Couette flow, Phys. Fluids 23 (6).

[34] D. S. Zimmerman, S. A. Triana, H.-C. Nataf, D. P. Lathrop, A turbulent, high magnetic Reynolds number experimental model of Earth's core, J. Geophys. Res. 119 (6) (2014) 4538–4557.

[35] D. Sweet, E. Ott, J. M. Finn, T. M. Antonsen, Jr., D. P. Lathrop, Blowout bifurcations and the onset of magnetic activity in turbulent dynamos, Phys. Rev. E 63 (2001) 066211.

[36] A. Alexakis, Y. Ponty, Effect of the Lorentz force on on-off dynamo intermittency, Phys. Rev. E 77 (2008) 056308.

[37] R. Raynaud, E. Dormy, Intermittency in spherical Couette dynamos, Phys. Rev. E 87 (2013) 033011.

[38] S. Childress, A. Gilbert, Stretch, Twist, Fold: the Fast Dynamo, Springer, 1995.

[39] F. Pétrélis, S. Fauve, Inhibition of the dynamo effect by phase fluctuations, Europhys. Lett. 76 (4) (2006) 602.